J Am Oil Chem Soc (2019)
DOI 10.1002/aocs.12269

ORIGINAL ARTICLE

Retardation of Crystallization through the Addition of Dairy Phospholipids

Zachary Cooper[1] · **Casey Simons**[2] · **Silvana Martini**[1]

Received: 14 March 2019 / Revised: 8 June 2019 / Accepted: 8 July 2019

Abstract The objective of this work was to identify the effects that milk phospholipids (PL) have on crystallization of anhydrous milk fat (AMF). Three mixtures were prepared by adding 0%, 0.01%, and 0.1% PL to AMF. Each mixture was crystallized for 90 min at 24, 26, and 28 °C. The solid fat content was measured as a function of time and fitted to the Avrami equation. Melting point, thermal behavior, viscoelastic properties, and crystal morphology were all measured at 90 min. All assays were repeated, as well as hardness, after being stored at 5 °C for 48 hours. Samples containing PL showed slower crystallization as concentration increased especially at higher temperatures (26 and 28 °C). The addition of PL caused a difference in crystal morphology resulting in visibly larger crystals at 90 min. The elasticity and hardness at 90 min were influenced by the addition of PL at 24 °C with lower values obtained in samples with PL compared to the AMF alone. No differences in hardness nor in elasticity was observed for samples crystallized at 26 and 28 °C. A decrease in melting enthalpy was observed in samples with PL indicating a reduction in crystallization at all temperatures, which was supported by crystal morphology.

Keywords Crystallization · Phospholipids · Milk · Solid fat content · Crystal morphology · Hardness · Elasticity

✉ Silvana Martini
silvana.martini@usu.edu

[1] Department of Nutrition, Dietetics, and Food Sciences, Utah State University, 8700 Old Main Hill, 750 N 1200 E, Logan, UT 84322, USA

[2] Department of Chemistry and Biochemistry, Utah State University, 8700 Old Main Hill, 750 N 1200 E, Logan, UT 84322, USA

J Am Oil Chem Soc (2019).

Introduction

Polar lipids are highly used and needed in the food industry. The most common polar lipids in the industry are known as phospholipids (PL), which consist of a lipid with a glycerol backbone, two fatty acid chains, and a phosphate group. PL are used for their emulsifying properties and to provide stability to food systems (Ahmad and Xu, 2015). For a long time, polar lipids have been known to exist in milk, but their concentration in milk is minimal (12.8–-40 mg L^{-1}) (Ahmad and Xu, 2015). Currently, products obtained from the dairy industry that are high in polar lipids are used as animal feed, low profit by-products, or are reworked into different product processes at low concentrations. Some of these products that are high in polar lipids come from butter serum, which is a low profit by-product from butter and butter oil manufacturing, and the isolated fat portion from the manufacturing of whey protein isolate (Ahmad and Xu, 2015).

In the food industry, there are various dairy PL products. These products are produced by various companies and generally come in a powdered form. PL products are produced to be ingredients and their PL content can range from as little as 20% PL and as much as 75% PL. Other components that may be included in these products are other lipids, lactose, and minerals.

Milk polar lipids have a different composition than common polar lipids that are currently used in the industry. The most common products that contain PL are from sources such as soy, sunflower, or egg and these polar lipids are commonly referred to as lecithins. According to the US

Code of Federal Regulations (CFR), Title 21 Volume 3 a "commercial lecithin is a naturally occurring mixture of the phosphatides of choline, ethanolamine, and inositol, with smaller amounts of other lipids" (CFR 21). There are various grades of lecithin including crude, fluidized, highly filtered, compound, chemically modified, and fractionated lecithins. Crude lecithins are often the grades of lecithin manufacturers produce. These products are standardized by usually using oil from the lecithin source to result in a consistent percentage of PL. CFR 21 does not give any limits to how much oil can be added, but soy lecithin can have as much as 40% triacylglycerols (TAG) and egg lecithin can have as little as 15%. For soy lecithin, the next grade would require to have less than 3% of TAG. This means that most lecithins used in the industry do not contain only PL. The literature shows that the polar lipid composition in soy lecithin is 32% phosphatidylcholine (PtdCho), 23% phosphatidylethanolamine (PtdEtn), 21% phosphatidylinositol (PtdIns), and 9% phosphatidic acid (PtdOH). In sunflower lecithin, the polar lipid composition is 34% PtdCho, 17% PtdEtn, 30% PtdIns, and 6% PtdOH (van Nieuwenhuyzen and Tomás, 2008). Sphingomyelin (CerPCho) and phosphatidylserine (PtdSer) are polar lipids that are not commonly reported in soy or sunflower lecithins due to their low concentration but these PL are usually found in animal-based lecithins (<1%) (Wendel, 2014). CerPCho is found in both egg (1.7%) and milk PL (26.8%), but PtdSer is not found in egg lecithin and can be only found in milk (1.5%). For example, the composition of egg polar lipids is approximately 79% PtdCho, 17% PtdEtn, 0% PtdIns, 0.3% PtdOH, 1.7% CerPCho, and 0% PtdSer (Sotirhos et al., 1986). In milk, the observed composition is 26.8% PtdCho, 25.8% PtdEtn, 14% PtdIns, 0.5% PtdOH, 26.8% CerPCho, and 1.5% PtdSer (Murgia et al., 2003).

Lecithins are commonly used as emulsifiers, to modify the viscosity of fluids, such as melted chocolate, and as a processing aid (van Nieuwenhuyzen and Tomás, 2008). Current research topics using lecithins include their use as encapsulating nutrients or pharmaceuticals in a lecithin-based mixture (Human et al., 2019), creating organogels with vegetable oils (Sato, 2018), and to control crystallization. The effects of lecithin on lipid crystallization show that lecithins do not influence the solid fat content (SFC) of nontrans-fat spreads with confectionary application, but they do influence the viscoelastic properties specifically increasing the elastic properties (Lončarević et al., 2013). In other studies, using cocoa butter, an induction of crystallization, affecting the SFC, occurred when soybean lecithin was added at low concentrations (0.2%) but as the concentration of PL increased, the rates of crystallization decreased (Miyasaki et al., 2016). A contrary effect was observed by Rigolle et al. (2015) in cocoa butter showing a delay in crystallization when sunflower and soy lecithin were added. When Smith (2000) observed the effects of PL on palm oil, it was found that nucleation was delayed with the addition of PL resulting in the formation of large spherulitic crystals. When a delay is observed with the addition of PL, the hypothesis is that PL are adsorbed onto the growth sites of the crystals (Vanhoutte et al., 2002) delaying the incorporation of TAG into the crystalline matrix. Overall the addition of lecithins or PL to lipid systems can cause different results depending on the source of the lecithin or PL and also on the processing conditions used (Lončarević et al., 2013). Fedotova and Lencki (2008) observed the influence that PL had in milk fat crystallization during butter making. When PL were added in the form of globular milk fat to reach a concentration of 0.66% PL, spherulite formation was inhibited. However, when adding soy lecithin at a level of 1.0%, spherulitic growth was stimulated until 2.0% lecithin was reached, which resulted in a broken up network. Overall, previous studies suggest that different combinations of fats and lecithins can induce, retard, or have no effect on crystallization. The percentage of lecithin in a fat may also show varying crystallization patterns as the concentration of lecithin or PL is increased.

Studies discussed above that evaluate the use of lecithins to change the crystallization behavior of fats either use vegetable lecithins or pure PL. No studies were performed with milk-based lecithins. Milk polar lipids offer a potential new functionality due to higher PtdSer levels compared to plant-based lecithins and the presence of CerPCho. Therefore, the objective of this research was to identify if milk PL would influence the crystallization behavior of anhydrous milk fat (AMF) and to characterize the physical properties of the crystalline network formed.

Materials and Methods

Materials

Phospholipids (PL) were isolated from a commercial source of PL concentrate (PC700, Fonterra, Auckland, New Zealand) using the method described below. The chemical composition of the PC700 as provided by the specification sheet was: 85.0% total lipids with 59.2% of PC700 being composed of PL. The lipid fraction of PC700 was composed of 3.0% phosphatidylserine (PtdSer), 31.0% phosphatidylcholine (PtdCho), 8.7% phosphatidylethanolamine (PtdEtn), and 16.5% sphingomyelin (CerPCho). PC700 also contained 2.5% moisture, 6.6% lactose, and a maximum content of 12.0% ash.

PL Extraction

The extraction of PL from the PC700 was performed by creating a suspension of the PC700 in water and then

precipitating out the PL using ethanol. Preliminary experiments in our laboratory have shown that the highest yield of PL was obtained with a 30:70 ratio of PC700:water. PC700 and the water were mixed using a magnetic stir bar in a beaker on a magnetic plate set to 1100 RPM for 30 min at ambient temperature forming an emulsion. The emulsion was then separated into four beakers of 25 g, placed on a magnetic stir plate with a stir bar set to 700 RPM, and ethanol was added to obtain a 1:2 emulsion: ethanol ratio by weight. The sample was stirred for 1 min after the ethanol was completely added and then given 5 min to rest while an agglomerate or precipitant formed. The ethanol: emulsion mixture was then vacuum filtered using a Büchner funnel and 47 mm diameter microfiber glass filter paper and vacuum. This process allowed separating the agglomerate from the rest of the materials in PC700. The PL agglomerate (PLA) was scraped off the filter paper and was placed on watch glasses under a hood for at least 36 hours to evaporate the ethanol. Samples were stored at 5 °C until the PLA was obtained.

Hexane Phospholipid Agglomerate Purification

The PLA obtained from the previous step still contained some impurities, presumably, minerals. Therefore, a purification step was performed using hexane. The hexane PLA purification was performed by making a 1:9 ratio of the agglomerate obtained from the previous step and hexane (AOCS Official Method Ja 3-87). The agglomerate was weighed in an Erlenmeyer flask and placed on a magnetic stir plate with a magnetic stirrer bar. The Erlenmeyer was covered with aluminum foil to minimize evaporation. The sample was agitated for 10–15 min until the agglomerate had dissolved in the hexane leaving a solid residue suspended in the media. The suspension was then poured into two 15 mL centrifuge tubes, passing a wash of hexane over the Erlenmeyer flask to remove any residuals of the hexane and sample bringing both 15 mL centrifuge tubes to a final volume of 6 mL. Samples were then centrifuged (IEC Centra CL3R, Thermo Electron Corporation, Waltham, MA, USA) using an 809 rotor at 1000 ×*g* and at 24 °C for 5 min. A white sediment could be seen at the bottom of the centrifuge with a yellow transparent solution on top. The supernatant was separated from the sediment and was transferred into a beaker. The centrifuge tubes were then brought up to a 4.5 mL volume using hexane to wash the sediment and improve the recovery of PL and vortexed until the sediment was brought back into solution. The samples were then centrifuged again, and the supernatant was transferred to the beaker as previously described. This washing process was performed three times. The centrifuge tubes and the beaker were then left under a hood for at least 12 hours until the hexane evaporated off. The obtained material after evaporation will be referred to as phospholipid isolate (PLI). The process to obtain PLI (extraction and purification processes) was repeated four times. All replicates were mixed and used for the NMR characterization described below and added to the AMF.

Thin Layer Chromatography (TLC)

The purity of the PL obtained after isolation was evaluated by doing TLC. TLC was performed in duplicate on four replicates of the PLI to ensure that the total PL concentration was consistent in each extraction. TAG, cholesterol, PtdCho, free fatty acids (FFA), cholesterol esters (CE), monoacylglycerols, 1–2 diacyglycerols, 1–3 diacylglycerols, and standards were also ran to be able to identify all of the compounds in the sample. A TLC plate (20 × 20 cm silica gel, 60 A particle, 250 μm layer) (Whatman, Little Chalfont, Bucks, UK) was prewashed and developed using a 100 mL mixture of chloroform and methanol at a 1:1 ratio by volume, then activated in the oven at 100 °C for 10 min. The PL (2.5 mg) samples were dissolved in 10 μL of Folch Solution (2:1 $CHCl_3$:MeOH 0.01% Butylated hydroxytoluene), dried using nitrogen gas, and then dissolved in 10 μL of Folch Solution and were placed 1 cm from the bottom of the plate and the plate was air dried. Once the plate was dried, it was sprayed with a 10% w/v cupric sulfate solution in 8% w/v orthophosphoric acid until it became translucent (Baron and Coburn, 1984). The plate was heated in an oven at 145 °C for 10 min (Churchward et al., 2008). A picture was taken of the plate using a Nikon d810 Camera (2014 Ayutthaya, Thailand) and analyzed using Image Lab 6.0.1(2017 Bio-Rad Laboratories Inc., Hercules, CA). In this software, the picture color was first inverted, then the columns were identified individually. The bands and band size were identified and the pixel count and intensity were identified and given, allowing for the percentage of components in the sample to be identified. Peillard et al. (2019) used and developed a similar method to be able to quantify the amount volatile fatty acids in a sample using a similar software program.

Identification of PL through Nuclear Magnetic Resonance ^{13}P (^{31}P NMR)

^{31}P NMR was performed using a Bruker AVANCE III 500 MHz high-resolution spectrometer (Bruker, Karlsruhe, Germany) equipped with a Bruker Smart Probe. The proton spectra were recorded at 500.132 MHz and the phosphorous spectra were recorded at 202.456 MHz. The methods reported by Lehnhardt et al. (2001) and MacKenzie et al. (2009) were used. A detergent solution was prepared as follows: 1 g of sodium cholate (from Alfa Aesar) was dissolved in a 10 mL deuterium oxide (purchased from

Aldrich)/water solution (20/80% v/v). To this was added ethylenediaminetetraacetic acid disodium dehydrate (purchased from Mallinckrodt Pharmaceuticals) (1% w/w) and phosphonomethylglycine (from Frontier Scientific) (0.3 g L^{-1}). The pH was adjusted using a Mettler Toledo Seven Compack pH/ion S220 pH meter to 7.40 using a sodium hydroxide solution (0.02 M) and the solution became clear. Four samples of PL (20 mg) were mixed with detergent solution (750 µL). Sodium hydroxide was added to the remaining detergent solution to raise the pH to 8.51 and further four samples were made. All eight samples were sonicated using a Branson 2800 sonicator for 30 min. Samples were transferred into 5 mm diameter NMR tubes. Spectra were recorded at 25 °C using the following acquisition parameters: 196 acquisitions, 54 k data points, 5000 Hz sweep width, 5.4 s acquisition time, and a 3.5 s relaxation time. All ^{31}P spectra were obtained using inverse gated proton decoupling (Bruker: igzg) to minimize the nuclear Ovenhauser effect. A line broadening of 0.2 Hz was applied to the obtained spectra. The spectra were processed using MestReNova v12.0.2 from Mestrelab Research S.L. Zerofilling was performed to increase the number of data points to 64 k. Quantitative global spectra distribution using six improvement cycles was applied to help deconvolute the overlapping peaks. The analysis was done after isolating sufficient PL required to obtain the PL mixtures and their replicates.

Mixtures

PL were added to AMF at three different concentrations: 0% PL, 0.01% PL, and 0.1% PL. To improve the solubility of the PL in the AMF, PL was added to the AMF by first dissolving it in a hexane 1:9 ratio PL:hexane w/v under 700 RPM agitation. The PL in hexane solution was added to the melted AMF and mixed for 10 min at 700 RPM, left under the hood for 48 hours or until all the hexane had evaporated off. The evaporation process was performed at room temperature and heated every 4–6 hours to keep the sample liquid.

Crystallization Kinetics—SFC

The crystallization kinetics of the AMF with and without the addition of PL was measured by following the variation of SFC as a function of time. Each sample was melted in a microwave for 1.5 min or until liquid and placed in five tempered p-NMR tubes. The samples were then placed in an oven at 65 °C for 30 min. The tubes were then placed into a water bath that were held at the crystallization temperature (T_c) (24, 26, and 28 °C) for 90 min. SFC was measured for 90 min every 5 min from the moment the tube was placed in the water bath ($t = 0$) until SFC began to increase exponentially in which case SFC was measured every 2 min. When the SFC reached a plateau, SFC was measured every 5 min. The SFC was measured in triplicate runs using an NMR Minispec mq 20 analyzer (Bruker, Karlsruhe, Germany). After 90 min of crystallization, two tubes from each run were stored at 5 °C for 48 hours and the SFC was measured again after this storage period to evaluate how the crystalline matrix evolved during storage at a lower temperature.

The crystallization kinetics was quantified using the Avrami equation (Marangoni, 2005) (1).

$$\frac{\mathrm{SFC}(t)}{\mathrm{SFCmax}} = 1 - e^{-kt^n} \quad (1)$$

where SFC_{max} is the maximum of SFC reached when the sample reaches equilibrium, k is the rate of crystallization, t is the time, and n is the Avrami exponent, which describes the growth and nucleation of the crystals (Marangoni, 2005). GraphPad Prism 8.0.0 (GraphPad Software, San Diego, CA, USA) was used to fit the data to the Avrami equation.

Melting Point and Melting Behavior

The melting point and melting behavior of the crystallized samples were measured in triplicate using a differential scanning calorimeter (DSC) (DSC Q20; TA Instruments, New Castle, DE, USA). The melting points of the various AMF:PL mixtures were measured by heating 10–15 mg of the sample up to 80 °C for 30 min to erase any crystal memory; decreasing the temperature at a rate of 5 °C min^{-1} to −20 °C and keeping the sample isothermally at −20 °C for 90 min to allow complete crystallization of the sample. Finally, the sample was heated to 80 °C at a rate of 5 °C min^{-1}. The melting point was identified as the peak temperature (T_p) of the highest melting peak from the last heating ramp from −20 to 80 °C.

The melting behavior of the samples crystallized at 24, 26, and 28 °C was evaluated from the tubes used for SFC determination. After 90 min at T_c, a sample (10–15 mg) was taken from the NMR tube and placed in a Tzero hermetically sealed pan and placed in TA DSC Q20 (TA Instruments, New Castle, DE, USA). The initial temperature was the same as the T_c and then increased 5 °C min^{-1} until 80 °C was reached. From all DSC graphs, the onset temperature (T_{on}), the peak temperature (T_p), and change in enthalpy associated with the melting process (ΔH) were calculated.

Similar to the description for SFC, the melting behavior was also measured after storing the sample at 5 °C for 48 hours to evaluate how the crystalline matrix evolved during storage at a lower temperature. In this case, the

initial temperature in the DSC was 5 °C and the temperature increased at 5 °C min^{-1} until reaching 80 °C.

Crystal Size and Morphology

Crystal morphology was observed in each of the triplicate runs using a polarized light microscope (PLM) (Olympus BX 41, Waltham, MA, USA) using a ×10 magnification objective and a digital camera (model Infinity 2, Lumenera Scientific, Ottawa, ON, Canada). Pictures of the crystals were taken from the samples used to measure SFC after 90 min at T_c. Crystal microstructure was also measured after storing the sample at 5 °C for 48 hours. The crystal diameter was measured from the PLM using Image-Pro Plus version 7.0 software (Media Cybernetics, USA). All crystals with a diameter of <4 μm were identified as background and were excluded from the analysis of the data. The crystals measured at 48 hours were those that could be clearly identified as the crystals that formed at 90 min.

Viscoelasticity

The viscoelastic property of the samples was measured in triplicate using a rheometer (AR-G2, TA Instruments, New Castle, DE, USA). Samples were prepared by placing 30 g of sample in a 50 mL centrifuge tube and melted in a microwave for 2 min or until the sample became liquid. The sample was then placed in an oven for 30 min and then placed in a water bath held at T_c for 90 min. The viscoelastic properties were then measured by using a 40 mm diameter geometry that was held at T_c. δ, G', and G'' were recorded and each replicate was measured three times using a strain sweep step (0.001–10% strain) oscillatory procedure (1 Hz) with a gap ranging from 500–1500 μm depending on how liquid the sample was. The 50 mL centrifuge tube was then stored at 5 °C for 48 hours and an 8-mm core sample was taken from the centrifuge tube to measure the sample viscoelasticity. The parallel plate was set at 5 °C and an 8 mm diameter geometry was used. Each replicate was measured three times using the same procedure as the 90 min samples and a 1000 μm gap was used. The data used were taken from the linear region at the 0.1% strain.

Hardness

The hardness of the sample was measured in triplicate using a TA-XT Plus Texture Analyzer (Texture Technologies, Scarsdale, NY, USA). Samples were prepared by melting the mixture in the microwave for 3 min or until the sample was liquid and placing the sample in an oven at 65 °C for 30 min. The samples were then placed in 1 cm diameter disposable test tubes and placed in an incubator held at the T_c for 90 min. Samples were too soft to allow for hardness measurement after 90 min and therefore samples were stored at 5 °C for 48 hours. After this storage, samples were removed from the test tube, cut into 0.5 in height cylinder and tested for hardness using a 5 cm diameter cylindrical probe using a calibrated 5 kg load. Each experimental replicate was measured five times.

Polymorphism

The polymorphism of all AMF samples and 0.01% and 0.1% samples crystallized at 24 and 26 °C was identified using a X-ray diffraction (XRD) Philips X'Pert 3040 MPD (PANalytical, Almelo, The Netherlands) diffractometer system with a single PW3050/ 00 (θ/2-θ) goniometer. A Cu Kα radiation X-ray source was used along with a PW3123/ 00 Monochromator detector. The software required to utilize the equipment was X'Pert Data Collector (v2.0e) (PANalytical, Almelo, The Netherlands). The samples were crystallized using the same crystallization method used for viscoelasticity and at the 90 min mark, the crystals were vacuum filtered using a Büchner funnel and a 47 mm diameter microfiber glass filter paper, and a vacuum flask that was connected to a vacuum. When the crystals were dried (>10 min of filtration), they were placed on to an X-ray slide. After the analysis for 90 min, the slides were stored at 5 °C for 48 hours and analyzed once more.

Statistical Analysis

Statistical analysis was performed on parameters using two-way ANOVA and GraphPad Prism 8.0.0 (GraphPad Software) was the statistical software used for all of the statistical analyses at 90 min, excluding crystal diameter, and SFC at 48 hours. Statistical Analytical Software (SAS) Studio (2019, SAS Institute Inc., Cary, NC, USA) was used to do the remaining 48 hours analyses and the 90 min crystal diameter.

Results and Discussion

PL Composition

The results of the TLC showed that the PLI replicates contained an average of 55.1 ± 3.5% of PL and this value was not significantly different among replicates ($P = 0.0862$). Standards showed that the remaining components in the isolated PL were cholesterol (15.6 ± 0.9%), FFA (11.6 ± 1.8%), monoacylglycerols (0.9 ± 0.2%), 1–2 diacylglycerols (5.8 ± 0.4%), 1–3 diacylglycerols (3.4 ± 0.4±), TAG (4.3 ± 0.7%), and CE (3.3 ± 1.9%). Based on the PL content of this isolate,

AMF:PL mixtures were prepared to achieve 0.1 or 0.01% of PL in the AMF sample.

The PL composition of the isolated PL obtained from the ^{31}P NMR is shown in Table 1 and compared to the previously reported values. These results show that the PL obtained had a similar composition to other milk-based PL. Two types of PL that are usually neglected due to low concentrations were lysophosphatidylethanolamine (2LPE) (2.5 ± 0.3%) and lysophosphatidylcholine (2LPC) (1.0 ± 0.1%). These two PL still had the lowest concentration compared to the rest of the PL, but compared to the results from other researchers, an identifiable concentration was found. PtdEtn (37.3 ± 1.3%) was higher than the literature values (23.5–31.4%) while CerPCho concentration was the lowest (17.8 ± 1.0%) compared to other reported values (Table 1). PtdSer concentration (4.4 ± 0.2%) was within the literature values. PtdIns (4.0 ± 0.3%) was lower than values reported in the literature and the PtdCho concentration (29.3 ± 1.3%) was higher. A lot of these differences could be due to the results of different processing conditions. Differences in these concentrations might arise from the variability of sample source and/or extraction method of the PL (Ahmad and Xu, 2015).

Crystallization Kinetics and SFC

The SFC was plotted as a function of time during the 90 min of crystallization as can be seen in Fig. 1. As temperature and PL concentration increased, a slower crystallization was observed. Data shown in Fig. 1 were fit to the Avrami equation where SFC_{max}, k, and n were calculated and are reported in Table 2. The Avrami equation could not be fit to PL concentrations of 0.01% and 0.1% at 28 °C because the SFC curves did not follow a sigmoidal shape and a maximum SFC was never reached during the 90 min at T_c. The AMF crystallized at 28 °C and the 0.1% PL sample crystallized at 26 °C could be fit to the Avrami equation but R^2 of both samples was very low (R^2 = 0.74 and 0.36, respectively) and cannot be considered reliable (Table 2). The rate of crystallization (k) decreased as the concentration of PL increased with a decrease of two orders of magnitude for AMF crystallized with 0.1% PL at 24 °C and for AMF with 0.01% PL crystallized at 26 °C compared to their AMF counterparts. The SFC obtained after 90 min (Fig. 1) are considerably different. At 24 °C, the SFC at 90 min showed no significant difference between samples (10.98 ± 0.28%). The samples crystallized at 26 °C showed a significant difference between AMF and 0.01% PL (8.79 ± 0.35%) and 0.1% PL (3.71 ± 2.68%). Samples crystallized at 28 °C showed a significant difference between AMF (6.24 ± 0.30%) and samples that contained PL (0.14 ± 0.03%). These results show that as the concentrations of PL and temperature increased, the maximum SFC decreased. All samples for AMF and the sample at 0.01% crystallized at 24 °C had n values close to three suggesting either disk-like growth from sporadic nuclei or spherulitic growth from instantaneous nuclei. All other samples with the addition of PL that could be fit to the Avrami equation had n values close to four suggesting spherulitic growth from sporadic nuclei (Marangoni, 2012). Literature showed similar results when soy lecithin was added at a 0.2% level to cocoa butter, although the results showed less variation with all samples resulting in a mix of instantaneous disc structure or spherulitic spontaneous structures (Miyasaki et al., 2016). Vanhoutte et al. (2002) reported n values similar to the ones reported in our study for AMF with 0.01% PL crystallized at 24 °C, but the other samples with 0.01% PL and 0.1% PL that showed spherulitic growth from sporadic nuclei did not compare with Vanhoutte's results. Slight differences between Vanhoutte's and our results might be due to variations in processing conditions such as temperature (25 °C), PL concentration (PL% < 0.03%), and crystallization time (3 hours) but also to the type of PL used. While Vanhoutte's group used soy

Table 1 Composition of the phospholipid isolate (PLI) as determined by ^{31}P NMR compared to previously reported data

PLmol%	PLI	Murgia et al., 2003	Andreotti et al., 2006	MacKenzie et al., 2009	Garcia et al., 2012
2LPE[a]	2.5 ± 0.3			2.9 ± 0.2	-
CerPCho[b]	17.8 ± 1.0	26.8	24.2	21.0 ± 0.1	19.9
PtdEtn/Lac-PE[b]	37.3 ± 1.3	25.8	23.5	27.9 ± 0.2/3.4 ± 0.2	31.4
2LPC[b]	1.0 ± 0.1				0
PtdSer[a]	4.4 ± 0.2	1.5	3.6	4.0 ± 0.1	11.2
PtdIns[a]	4.0 ± 0.3	14.0	12	3.2 ± 0.2	3.6
PtdCho[b]	29.3 ± 1.3	26.8	24	30.6 ± 0.1	28.7

Data reported are the average of four analytical replicates. PL, phospholipid; 2LPtdEtn, lysophosophatidylethanolamine; CerPCho, sphingomyelin; PtdEtn, phosphatidylethanolamine; Lac-PtdEtn, lactosylated phosphatidylethanolamine; 2LPtdCho, lysophosphatidylcholine; PtdSer, phosphatidylserine; PtdIns, phosphatidylinositol; PtdCho, phosphatidylcholine; PLI, phospholipid isolate.

[a] PL species were obtained from solution with a pH of 8.5.

[b] PL species were obtained from solution with a pH of 7.4.

Table 2 Parameters obtained from the Avrami fitting performed in the SFC data reported in Fig. 1

	Temperature (°C)	AMF	AMF + 0.01% PL	AMF + 0.1% PL
SFC_{max} (%)	24	11.03 ± 0.11	10.24 ± 0.08	10.55 ± 0.18
	26	8.66 ± 0.09	8.17 ± 0.08	4.61 ± 4.04
	28	6.45 ± 1.70	N/A	N/A
k^{min-1}	24	$1.7 \times 10^{-4} \pm 1.0 \times 10^{-4}$	$2.4 \times 10^{-4} \pm 1.2 \times 10^{-4}$	$1.3 \times 10^{-6} \pm 1.6 \times 10^{-6}$
	26	$1.2 \times 10^{-5} \pm 5.7 \times 10^{-6}$	$2.5 \times 10^{-7} \pm 2.5 \times 10^{-7}$	$4.8 \times 10^{-11} \pm 8.2 \times 10^{-10}$
	28	$2.6 \times 10^{-5} \pm 7.0 \times 10^{-5}$	N/A	N/A
n	24	2.99 ± 0.21	2.66 ± 0.16	3.61 ± 0.34
	26	3.23 ± 0.14	4.03 ± 0.26	5.43 ± 4.22
	28	2.52 ± 0.76	N/A	N/A
R^2	24	0.96	0.97	0.94
	26	0.98	0.97	0.36
	28	0.74	N/A	N/A

lecithin, our work used milk-based PL. Based on the n values obtained in our research, it is possible that independent of the T_c used, the addition of PL induced the formation of spherulitic-shaped crystals. This type of crystal morphology is usually observed in slowly crystallized samples, which is the case of the PL-based samples (Martini et al., 2002). The SFC was also measured after 48 hours and no significant difference between the samples was observed (SFC = $45.0 \pm 0.6\%$; $P > 0.05$). The SFC after 48 hours being nonsignificantly different indicates that a secondary crystallization is occurring. This secondary crystallization would be due to the high super cooling that is introduced (5 °C) after 90 min, indicating that the samples with a lower SFC after 90 min (0.1% PL at 26 and 28 °C samples) may result in smaller crystals (Martini et al., 2002) influencing the properties of the crystalline network.

Overall, results show that the addition of milk PL delayed the crystallization of AMF. The melting point of AMF with and without PL was not statistically different with a T_p of 33.18 ± 0.13 °C. A difference in enthalpy was seen between the samples containing PL (71.1 ± 3.4 W g^{-1}) and the AMF sample (84.4 ± 1.6 W g^{-1}), which indicates that fewer crystals were formed during the crystallization with the addition of PL. Because the melting point of the samples was not affected by PL addition, it is likely that the delay in crystallization observed is due to changes that occur during crystallization at the molecular level. Previous studies have suggested that when molecules used as additives are similar to the TAG, as would be the case of PL, they can be incorporated into the crystalline matrix and delay crystal growth. It has been shown that minor components can play a role in the crystallization characteristics of lipids (Smith, 2000). The presence of monoacylglycerols and diacylglycerols in our PL isolate can also contribute to a delay in the crystallization as previously reported by Wright et al. (2000) and Wright and Marangoni (2003).

Crystal Morphology

Fig. 2 shows the morphology of crystals obtained for the samples. For the AMF samples crystallized at 24 °C, it is evident that crystallization occurs with the formation of instantaneous nuclei forming many disk- shaped crystals. The same behavior is observed for AMF crystallized at 26 °C but in addition to the disk-like crystals, traces of spherulitic crystals can be seen. Samples crystallized at 28 °C show clear spherulites. The addition of PL promoted the formation of spherulites. As the concentration of PL increased, spherulites became bigger in size. Smith (2000) also observed similar changes in the morphology of palm oil with PL. The results showed an increase in size with the addition of PL due to the retardation of nucleation and the stunting of crystallization. Another visible difference is the very distinct Maltese-cross that appears when PL is added. No crystals were observed for samples crystallized at 28 °C with the addition of 0.1% PL and the sample at 0.01% PL had few crystals at 90 min resulting in the crystals that formed after 48 hours were due to the secondary phase of crystallization during storage and not the crystallization temperature.

After measuring the crystal size diameter at both 90 min and 48 hours (Table 3), a trend was observed, whereas the diameter increased with concentration of PL and temperature. At 90 min, there was a significant difference between AMF (14.8 ± 2.2 μm) and samples containing 0.01% PL (54.2 ± 6.3 μm) and 0.1% PL (96.1 ± 2.2 μm) at 24 °C ($P < 0.0001$), while at 26 °C the only difference was seen between AMF (14.6 ± 3.4 μm) and 0.1% PL (118.4 ± 18.2 μm) ($P = 0.0020$). At 48 hours, all samples crystallized at 24 °C were significantly different from one another ($P < 0.001$), but the significant difference at 26 °C was only between AMF (20.57 ± 2.84 μm) and 0.1% PL (119.12 ± 20.83 μm) ($P = 0.0014$), similar to the 90 min

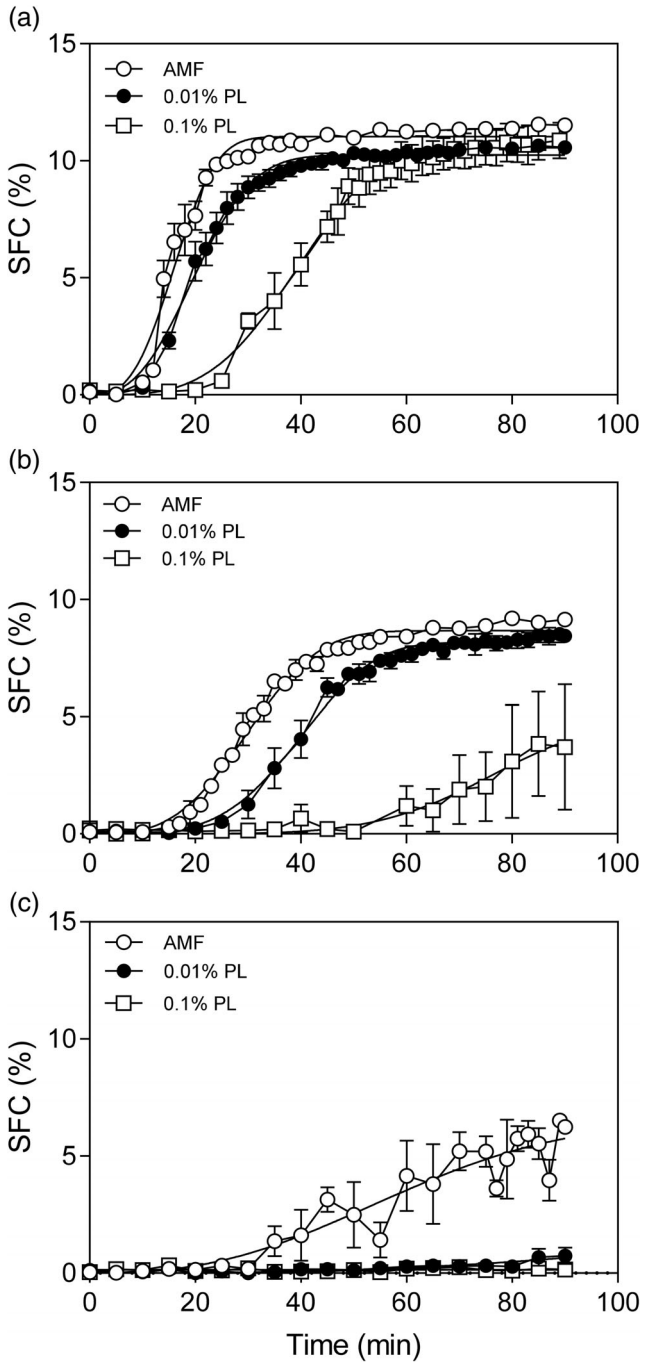

Fig. 1 SFC of samples (AMF, AMF + 0.01% PL, and AMF + 0.1% PL) as they crystallized over 90 min at 24 °C (a), 26 °C (b), and 28 °C (c)

sample. It is understood that as temperatures increase the crystallization rate decreases due to lower driving force for crystallization (Wright et al., 2000). The effect of retardation was due to both the addition of PL and an increase in temperature. This is also supported by Martini et al. (2002) in the theory that as the time it takes for crystals to form increases, the size of the crystals also increases.

It is interesting to note that the addition of PL not only changes the crystal size but also the crystal morphology. Changes in the crystal morphology could be due to difference in crystallization kinetics but also to different polymorphic forms. XRD analysis showed that AMF samples crystallized at 24, 26, and 28 °C formed a β' polymorphism with signals observed at 4.2 and 3.8 Å. When these samples were stored at 5 °C for 48 hours, a β polymorph was only observed for the sample crystallized at 28 °C that coexisted with the β' form (signals observed at 4.8, 4.2, and 3.8 Å). The addition of 0.01% PL induced the formation of a β and β' polymorph only for the sample crystallized at 24 °C with peaks detected at 4.6, 4.2, and 3.8 Å, but only the β' polymorphism was observed after 48 hours of storage at 5 °C. The addition of 0.1% PL to AMF crystallized at 24 °C induced the formation of β' polymorphism only with signals at 4.2 and 3.8 Å. The effect of PL addition to AMF crystallized at 26 °C was somewhat contrary to the one observed at 24 °C. The addition of 0.01% of PL generated β' polymorphs with signals at 4.2, 4.1, and 3.8 Å; while the addition of 0.1% of PL generated a mixture of β' and β polymorphs with signals at 4.8, 4.2, and 3.9 Å. These two polymorphic forms were maintained for the samples even after storage at 5 °C for 48 hours.

Melting Behavior

The DSC melting profiles are shown in Fig. 3 and the DSC parameters in Fig. 4. As expected, T_{on} increased with T_c ($P < 0.05$). The addition of PL increased T_{on} but this change was only significant for samples crystallized at 26 °C indicating that milk PL had a higher influence on crystallization at 26 °C than at other crystallization temperatures ($P < 0.05$). The reason for the significant difference at 26 °C could be that low-melting-point and high-melting-point TAG crystallize at this temperature while only high-melting-point TAG crystallize in the samples where PL was added increasing the T_{on}. Similarly, at 24 °C both low-melting-point and high-melting-point TAG have crystallized at 90 min resulting in a lower T_{on} that is not affected by the addition of PL due to the high degree of supercooling. When samples were crystallized at 28 °C, only high-melting TAG are crystallized resulting in a higher T_{on} that is not affected by the addition of PL. It is possible that at 26 °C, PL inhibit the crystallization of low-melting-point TAG but that this effect is not seen at 28 °C because low-melting-point TAG do not crystallize at this temperature even in the samples without the addition of PL due to the low supercooling. Similar results were observed by Daels et al. (2015) and Miyasaki et al. (2016) when they added 1.5% sunflower lecithin to vegetable fats and standard lecithin (0.2%, 0.5%, and 0.8%) to cocoa butter, respectively. No difference was seen in the DSC melting profiles with

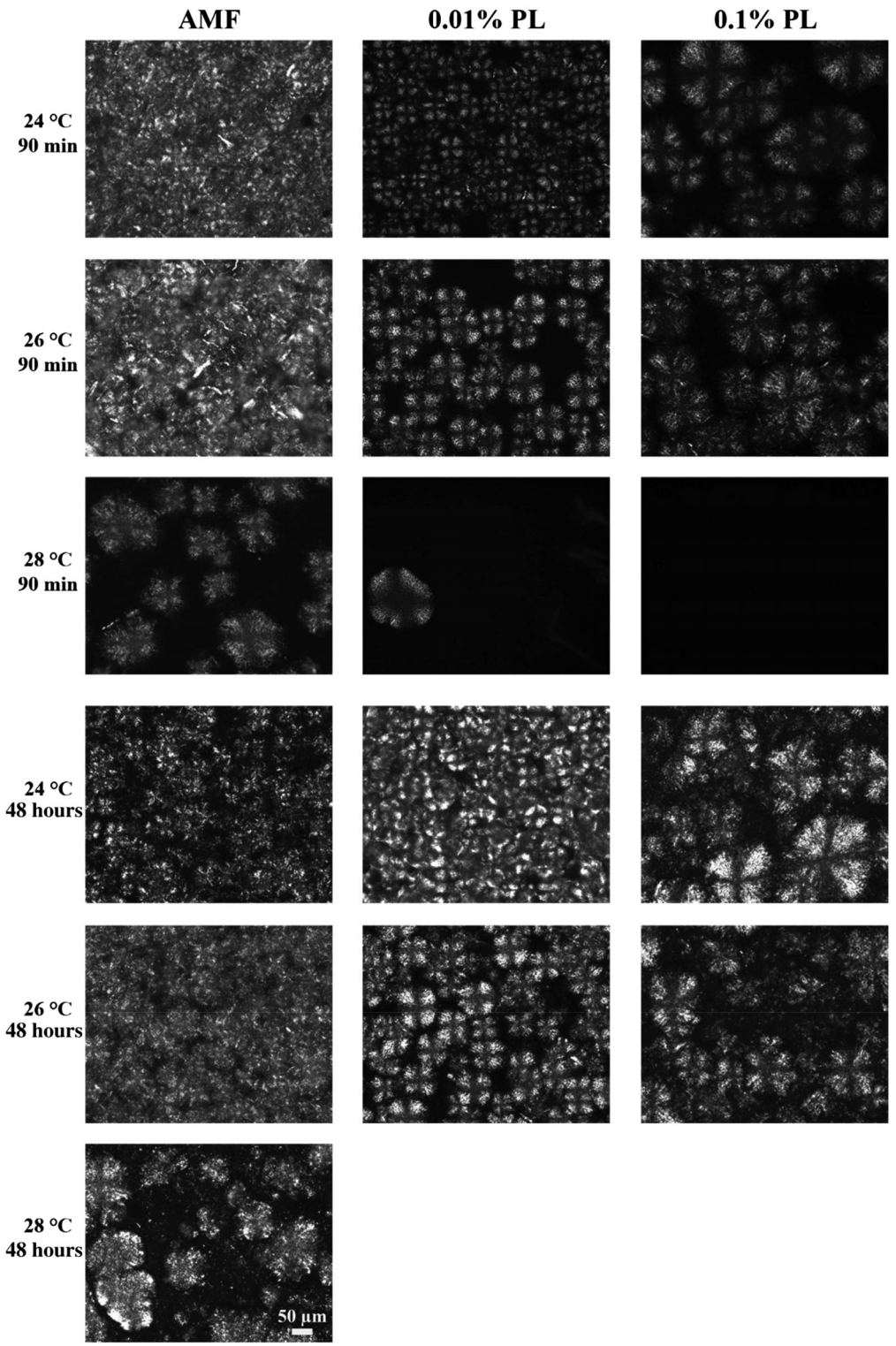

Fig. 2 Crystal morphology of all samples (AMF, AMF + 0.01% PL, and AMF + 0.1% PL) at 90 min at crystallization temperatures (24, 26, and 28 °C) and after being stored at 5 °C 48 hours

the addition of PL (Fig. 3) other than peaks were less defined for 90 min samples as PL increases. Contrary to the results shown by Miyasaki, there was no difference seen in T_p as the concentration of PL increased. Miyasaki observed that modified and unmodified soy lecithins decreased T_p of cocoa butter and this could easily be attributed to the cocoa

Table 3 Crystal diameters (μm) obtained from the PLM at 90 min after crystallization and after being stored at 5 °C for 48 hours

Time	Temp (°C)	AMF	AMF + 0.01% PL	AMF + 0.1% PL
90 min	24	14.80 ± 2.18d	54.20 ± 6.27ac	96.15 ± 2.20ab
	26	14.58 ± 3.43cd	75.59 ± 16.50abc	118.42 ± 18.20ab
	28	72.04 ± 8.89abcd	114.31 ± 30.98a	NA
48 hours	24	10.19 ± 0.06c	52.01 ± 6.12b	97.85 ± 6.52a
	26	20.57 ± 2.84bc	67.43 ± 7.48ab	119.12 ± 20.83a
	28	51.27 ± 22.51abc	N/A	N/A

Variables within the same time with the same letter are not significantly different ($\alpha = 0.05$). N/A = Data were not reported because no crystals were observed at 90 min.

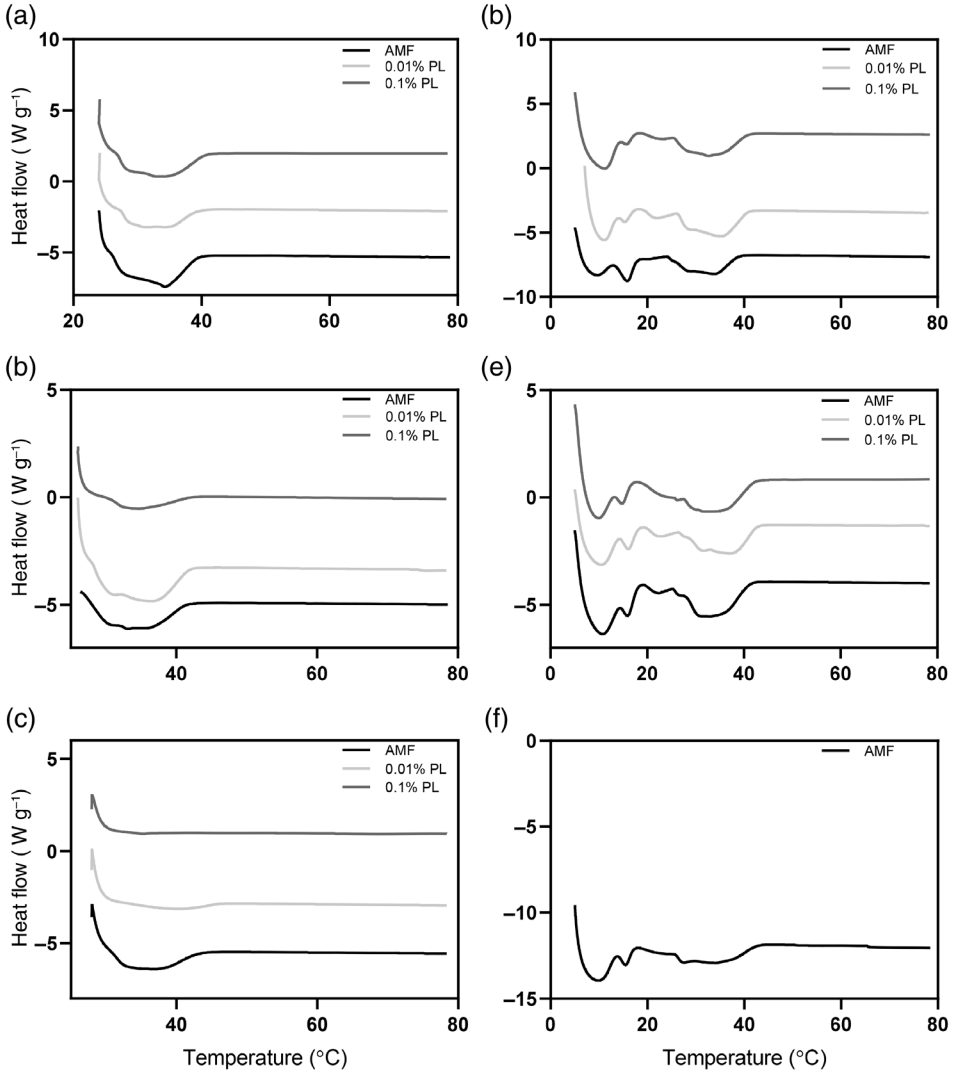

Fig. 3 Melting profiles of all samples (AMF, AMF + 0.01% PL, and AMF + 0.1% PL) at 90 min after crystallization temperatures 24 °C (a), 26 °C (b), and 28 °C (c). The samples were stored at 5 °C for 48 hours and the melting profile was analyzed for each of the samples crystallized at 24 °C (d), 26 °C (e), and 28 °C (f)

butter having many polymorphic forms. It was interesting to note that there was a significant difference in the enthalpy (ΔH) of the samples at 90 min. For samples crystallized at all T_c, a significant difference ($P < 0.05$) was observed between samples that contained PL and AMF. For samples crystallized at 24 °C, this difference was

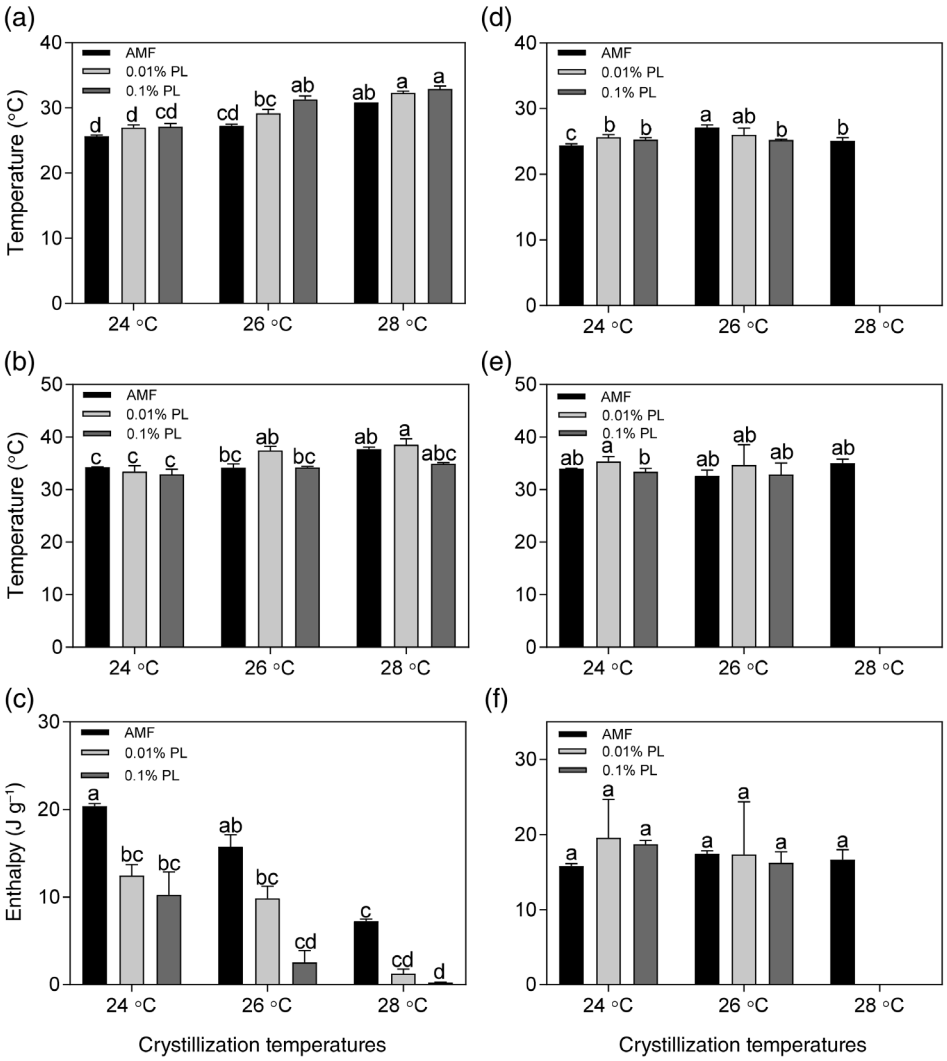

Fig. 4 Melting parameters T_{on} (a), T_p (b), and ΔH (c) of all samples (AMF, AMF + 0.01% PL, and AMF + 0.1% PL) at 90 min after crystallization temperatures (24, 26, and 28 °C). The samples were stored at 5 °C for 48 hours and the melting profile was analyzed for each of the samples from crystallization temperatures (24, 26, and 28 °C) for each of the parameters T_o (d), T_p (e), and ΔH (f). Data were analyzed using a Tukey multiple comparison two-way ANOVA test. Parameters within the same graph with the same letter are not significantly different ($\alpha = 0.05$)

significant even at low concentrations of PL (0.01%). These results suggest that as the amount of PL increased, crystallization was delayed, which is in agreement with the SFC (Fig. 1) values, and the crystal morphology (Fig. 2) previously described. Smith (2000) also observed a reduction in nucleation and crystallization when he added soy lecithin and PL to palm oil. The crystallization kinetics previously discussed shows that as the PL concentration increased crystallization was delayed, which means fewer crystals would be present at 90 min requiring less energy to melt the crystals that had formed (Foubert et al., 2008). Literature also suggests that as enthalpy increases, it indicates homogeneity throughout the crystals creating a more interactive crystal lattice (Arishima et al., 1995; Macmillan et al., 2002; Seguine, 1991; Svanberg et al., 2013). After 48 hours of storage at 5 °C, two melting peaks were observed (Fig. 3): one melting peak that occurred at low temperatures (below 20 °C) and a second melting peak that occurred at higher temperatures (above 20 °C). The T_{on}, T_p, and enthalpy values reported in Fig. 4d, e, and f are the ones obtained for the high-temperature melting peak because this peak is the one that represents that crystals formed during crystallization at T_c for 90 min. Note that melting parameters of samples crystallized with PL at 28 °C were not reported after storage at 5 °C. Because these samples showed little to no crystallization for 90 min at T_c, the results obtained after storing samples at 5 °C will not provide any additional information to our results. We expect that small crystals will be formed due to the high supercooling that do not contribute to the study of

isothermal crystallization events discussed in this research. A significant difference was observed for T_{on} and T_p at 48 hours. T_{on} of AMF samples crystallized at 24 °C with PL significantly increased from 24.37 ± 0.16 °C for AMF, 25.66 ± 0.23 °C for AMF with 0.01% PL and 25.29 ± 0.16 °C for AMF with 0.1% PL. Although there is not a significant difference at 90 min, there is a similar trend that is shown, which indicates that the T_{on} at 48 hours could have been highly influenced by the crystals that form at 90 min. At 26 °C, a significant decrease between the T_{on} of the AMF sample (27.15 ± 0.22 °C) and the 0.1% PL sample (25.21 ± 0.07 °C) was observed. This is an opposite trend compared to the one observed at 90 min at 26 °C. It is possible that the lack of crystals produced at 26 °C in the 0.1% PL sample over 90 min allows for the remaining liquid oil to create smaller crystals that may be less stable and melt faster resulting in a lower temperature T_{on}. The T_p showed a significant decrease between PL samples crystallized at 24 °C at 48 hours from 35.37 ± 0.55 °C to 33.40 ± 0.37 °C for the 0.01% PL with 0.1% PL samples, respectively. This would be due to an interaction effect of the PL and temperature because it can only be seen at this temperature and not the others. The enthalpy after 48 hours of storage showed no significant difference between samples ($P > 0.05$).

Hardness

The hardness was measured after storage at 5 °C for 48 hours. Statistical differences were observed at 24 and 26 °C. The samples at 28 °C that contained PL were not included due to the fact that a crystallization occurred due to the storage temperature rather than the T_c. During this secondary crystallization, many small crystals were formed that contributed to the harder crystalline network for samples that had lower final SFC at 90 min (Fig. 2). The trends show that the hardest sample was obtained at 24 °C AMF (20.09 ± 1.46 N) followed by 0.1% PL (15.39 ± 0.89 N) and by the 0.01% PL sample (13.08 ± 0.55 N). Only the AMF sample and 0.01% PL sample were significantly different at 24 °C ($P = 0.0007$). Even though a tendency of higher hardness was observed at 0.1% PL addition vs. 0.01% PL addition, these differences were not significant ($P > 0.05$, Fig. 5). The decrease in hardness as a function of PL addition observed at 24 °C is due to the delay in crystallization and the increase in crystal sizes previously discussed. At 26 °C, the trend changed with the sample at 0.1% PL level being the hardest (25.62 ± 2.10 N), followed by AMF (20.11 ± 0.81 N) and then 0.01% PL (16.73 ± 0.88 N). This trend supports a theory that when a sample with a low SFC is stored at 5 °C for 48 hours, a secondary crystallization occurs causing a small crystalline network resulting in harder samples.

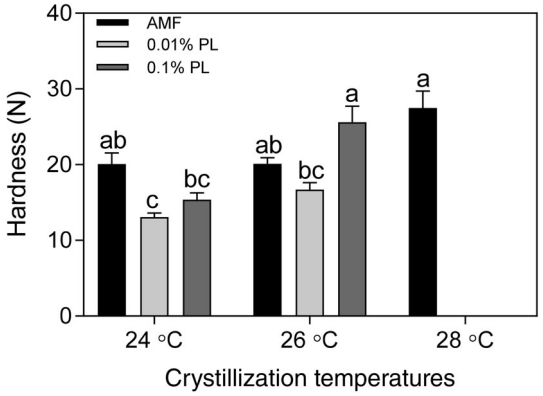

Fig. 5 Hardness of all samples (AMF, AMF + 0.01% PL, and AMF + 0.1% PL) after being crystallized for 90 min at crystallization temperatures (24, 26, and 28 °C) and being stored at 5 °C for 48 hours. The data were analyzed using a Tukey multiple comparison two-way ANOVA test. Samples with the same letter are not significantly different ($\alpha = 0.05$)

A significant difference at 26 °C was only observed between the 0.1% PL sample and the 0.01% PL sample ($P = 0.0011$).

Viscoelasticity

Hardness data are difficult to interpret, especially for the samples crystallized at 28 °C and at 26 °C with the addition of PL because the secondary crystallization that occurs during storage might confound the results obtained. Therefore, measuring the viscoelasticity after the 90 min of crystallization might be a better measurement to evaluate how PL addition affects the elasticity of the sample. As the T_c increased, the elastic modulus decreased due to the lack of crystals in the sample (Fig. 6). The only temperature that showed a difference between PL addition was 24 °C where the addition of PL resulted in a decreased G' ($P < 0.05$). This could be due to the crystallization kinetics previously described. When PL were added to the sample, crystallization was slowed down causing fewer crystals to be present compared to the AMF sample. When looking at the PLM of the AMF samples crystallized at 24 °C, more diverse crystals were observed in AMF samples compared to the ones observed in samples with PL. G' values reported for samples crystallized at 24 °C follow the same trend as the hardness values previously discussed (Fig. 5). G' values of samples crystallized at 26 °C followed the same trend that was observed with the hardness values at 26 °C. The viscous modulus (G'') showed similar trends to the ones described for G' while no significant differences were observed for the delta values. After 48 hours of storage at 5 °C, G' values increased but showed no significant difference. Even after storage at 5 °C, lower G' values were

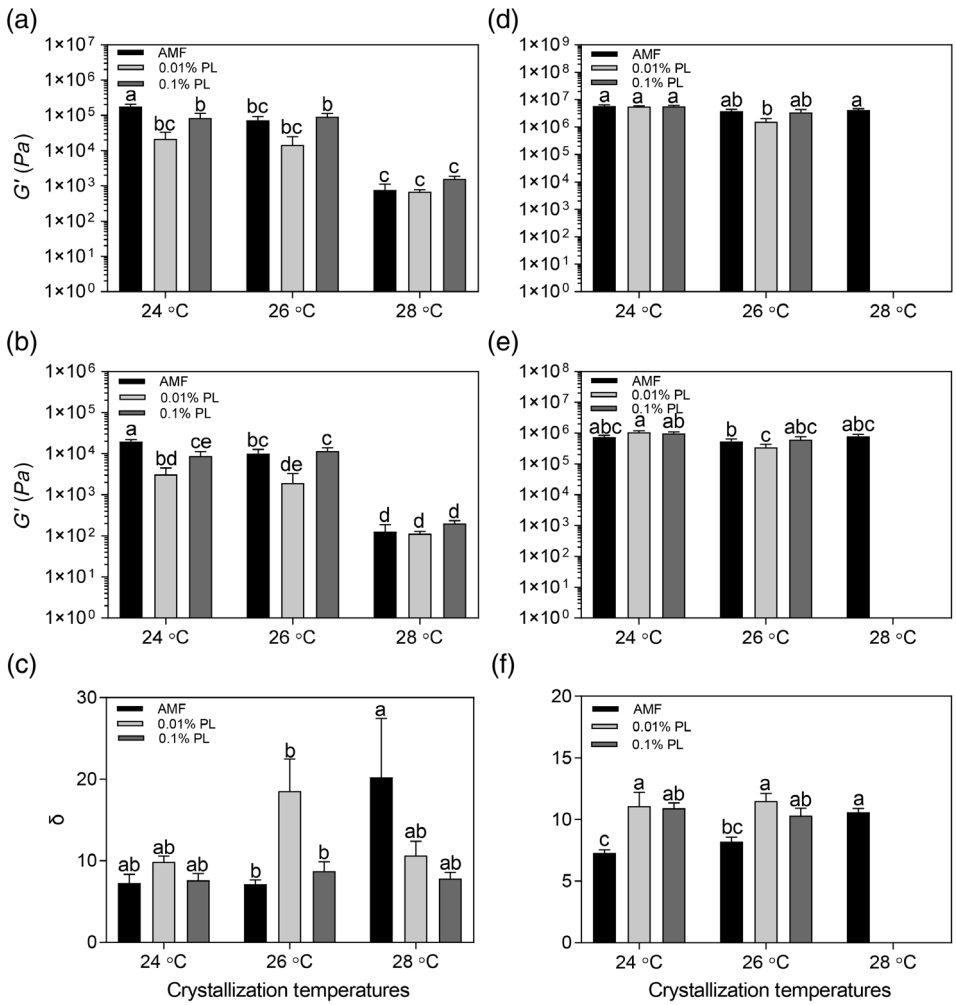

Fig. 6 Viscoelastic parameters G' (a), G'' (b), and δ (c) of all samples (AMF, AMF + 0.01% PL, and AMF + 0.1% PL) at 90 min after crystallization temperatures (24, 26, and 28°C). The samples were stored at 5 °C for 48 hours and the viscoelastic behavior was measured for each of the samples (d, e, and f). Data was analyzed using a Tukey multiple comparison two-way ANOVA test. Parameters within the same graph with the same letter are not significantly different ($\alpha = 0.05$)

observed for samples crystallized at higher T_c but no effect on G' values was observed due to PL addition. Among samples stored for 48 hours, no significant difference in G'' was observed other than at 26 °C where AMF ($5.39 \times 10^5 \pm 1.03 \times 10^5$ Pa) showed a higher G'' than 0.01% PL ($3.44 \times 10^5 \pm 9.92 \times 10^4$ Pa). This trend is the same trend reflected at 90 min, but shows a smaller difference between samples suggesting that during storage the growth of the crystals from liquid oil helped to decrease the differences between the PL samples and AMF.

Conclusion

The addition of milk PL retarded crystallization growth and reduced the amount of crystals that could be grown within 90 min. As the temperature increased, the effect of PL on the delay of crystallization increased. The low concentrations of PL (0.01%) had a significant effect in terms of G', G'', the 90 min enthalpy required to melt the sample, and the 48 hours T_{on} at 24 °C, G'' also showed to be lower at 26 °C at 90 min and 48 hours, and the SFC at 90 min at high temperatures (28 °C). The 0.1% PL sample showed a significant effect on the SFC at 90 min above room temperature (26 and 28 °C), a decrease in the 90 min enthalpy at all temperatures, an increase in the T_{on} at 90 min, but a decrease in the T_{on} at 48 hours at 26 °C, an increase in the 48 hours T_o at 24 °C, and a decrease in the G'' at 90 min compared to AMF. The addition of PL also influenced nucleation and the crystal growth form. All these factors were due to the physical properties of the crystals, which were related to how the PL interacted with the crystals

during crystallization, at 90 min, and as the samples were stored. The hardness after 48 hours was influenced by the size, or lack thereof, of the crystals developed during the 90 min of crystallization. Overall, it can be concluded that milk PL cause a delay in crystallization due to interaction that PL have with the crystals during crystallization.

Acknowledgments We are very grateful for the donations of PC700 from Frontera, funding from the BUILD Dairy Program, Dr. Robert Ward's laboratory at Utah State University for the guidance on thin layer chromatography, and the National Science Foundation MRI-1429195 grant that assisted in the funding of the Bruker 500 MHz NMR. This research was supported by the Utah Agricultural Experiment Station, Utah State University, and approved as journal paper number 9192.

Conflict of Interest The authors declare that they have no conflict of interest.

References

Ahmad, M. U., & Xu, X. (2015) *Polar lipids biology, chemistry, and technology*. Chicago, IL: AOCS Press.

Andreotti, G., Trivellone, E., & Motta, A. (2006) Characterization of buffalo milk by ^{31}P-nuclear magnetic resonance spectroscopy. *Journal of Food Composition and Analysis*, **19**:843–849.

Arishima, T., Sagi, N., Mori, H., & Sato, K. (1995) Density measurement of the polymorphic forms of POP, POS and SOS. *Journal of Japanese Oil Chemists Society*, **44**:431–437.

Baron, C. B., & Coburn, R. F. (1984) Comparison of two copper reagents for detection of saturated and unsaturated neutral lipids by charring densitometry. *The Journal of Liquid Chromatography*, **7**: 2793–2801.

Churchward, M. A., Brandman, D. M., Rogaseveskaia, T., & Coorssen, J. R. (2008) Copper (II) sulfate charring for high sensitivity on-plate fluorescent detection of lipids and sterols: Quantitative analyses of the composition of functional secretory vesicles. *Journal of Chemical Biology*, **1**:79–87.

Daels, E., Rigolle, A., Raes, K., Block, J. D., & Foubert, I. (2015) Monoglycerides, polyglycerol esters, lecithin, and their mixtures influence the onset of non-isothermal fatcrystallization in a concentration dependent manner. *European Journal of Lipid Science and Technology*, **117**:1745–1753.

Fedotova, Y., & Lencki, R. W. (2008) The effect of phospholipids on milkfat crystallization behavior. *Journal of American Oil Chemists' Society*, **85**:205–212.

Foubert, I., Fredrick, E., Vereecken, J., Sichien, M., & Dewettinck, K. (2008) Stop-and-return DSC method to study fat crystallization. *Thermochimica Acta*, **471**:7–13.

Garcia, C., Lutz, N. W., Confort-Gouny, S., Cozzone, P. J., Armand, M., & Bernard, M. (2012) Phospholipid fingerprints of milk from different mammalians determined by ^{31}P NMR: Towards specific interest in human health. *Journal of Food Chemistry*, **135**: 1777–1783.

Human, C., Beer, D. D., Rijst, M. V. D., Aucamp, M., & Joubert, E. (2019) Electrospraying as a suitable method for nanoencapsulation of the hydrophilic bioactive dihydrochalcone, aspalathin. *Journal of Food Chemistry*, **276**:467–474.

Lehnhardt, F. G., Röhn, G., Ernestus, R. I., Grüne, M., & Hoehn, M. (2001) ^{1}H- and ^{31}P-MR spectroscopy of primary and recurrent human brain tumors *in virto*: Malignancy-characteristic profiles of water soluble and lipophilic spectral componenets. *NMR in Biomedicine*, **14**:307–317.

Lončarević, I., Pajin, B., Omorjan, R., Torbica, A., Zarić, D., Maksimović, J., & Gajić, J. Š. (2013) The influence of lecithin from different sources on crystallization and physical properties of non-trans fat. *Journal of Texture Studies*, **44**:450–458.

MacKenzie, A., Vyssotski, M., & Nekrasov, E. (2009) Quantitative analysis of dairy phospholipids by ^{31}P NMR. *Journal of American Oil Chemists Society*, **86**:757–763.

Macmillan, S. D., Roberts, K. J., Rossi, A., Wells, M. A., Polgreen, M. C., & Smith, I. H. (2002) In situ small angle X-ray scattering (SAXS) studies of polymorphism with the associated crystallization of cocoa butterfatusingshearingconditions. *Crystal Growth and Design*, **2**:221–226.

Marangoni, A. G. (2005) *Fat crystal networks*. New York, NY: Marcel Dekker.

Marangoni, A. G. (2012) *Structure-function analysis of edible fats*. Chicago, IL: AOCS Press.

Martini, S., Herrera, S. L., & Hartel, R. W. (2002) Effect of cooling rate on crystallization behavior of milk fat fraction/sunflower oil blends. *Journal of American Oil Chemists' Society*, **79**:1055–1062.

Miyasaki, E. K., Luccas, V., & Kieckbusch, T. G. (2016) Modified soybean lecithins as inducers of the acceleration of cocoa butter crystallization. *European Journal of Lipid Science and Technology*, **118**:1539–1549.

Murgia, S., Mele, S., & Monduzzi, M. (2003) Quantitative characterization of phospholipids in Milk fat via ^{31}P NMR using a monophasic solvent mixture. *Lipids*, **38**:585–591.

Peillard, F. R., Mattio, E., Komino, A., Boudenne, J. L., & Coulom, B. (2019) Develompnt of a simple, l02-cost and rapid thin layer chromatography method for determination of individual volatile fatty acids. *The Royal Society of Chemistry*, **11**:1891–1897.

Rigolle, A., Gheysen, L., Depypere, F., Landuyt, A., Abeele, K., & Foubert, I. (2015) Lecithin influences cocoa butter crystallization depending on concentration and matrix. *Europena Journal of Lipid Science and Technology*, **117**:1722–1732.

Sato, K. (2018) *Crystalliztion of lipids*. Hoboken, NJ: Wiley.

Seguine, E. S. (1991) Tempering the inside story. *Journal of Manufufacterers Confectionary*, **71**:117–125.

Smith, P. R. (2000) The effects of phospholipids on crystallisation and crystal habit in triglycerides. *European Journal of Lipid Science and Technology*, **102**:122–127.

Sotirhos, N., Herslöf, B., & Kenne, L. (1986) Quantitative analysis of phospholipids by $_{31}$P-NMR. *Journal of Lipid Research*, **27**: 386–392.

Svanberg, L., Ahrné, L., Lorén, N., & Windhab, E. (2013) Impact of pre-crystallization process on structure and product properties in dark chocolate. *Journal of Food Enginineering*, **114**:90–98.

van Nieuwenhuyzen, W., & Tomás, M. C. (2008) Update on vegetable lecithin and phospholipid technologies. *European Journal of Lipid Science and Technology*, **110**:472–486.

Vanhoutte, B., Foubert, I., Duplacie, F., Huyghebaert, A., & Dewettinck, K. (2002) Effect of phospholipids on isothermal crystallisation and fractionation of milk fat. *European Journal of Lipid Science and Technology*, **104**:738–744.

Wendel, A. (2014) *Kirk-Othmer encyclopedia of chemical technology, lecithin*. Hoboken, NJ: John Wiley & Sons.

Wright, A. J., Hartel, R. W., Narine, S. S., & Marangoni, A. G. (2000) The effect of minor Componenets on Milk fat crystallization. *Journal of the American Oil Chemists Society*, **77**:463–475.

Wright, A. J., & Marangoni, A. G. (2003) The effect of minor components on Milk fat microstructure and mechanical properties. *Journal of Food Science*, **68**:182–186.